

# Identification of the specific microRNAs and competitive endogenous RNA mechanisms in osteoporosis

Journal of International Medical Research

48(10) 1–15

© The Author(s) 2020

Article reuse guidelines:

[sagepub.com/journals-permissions](http://sagepub.com/journals-permissions)

DOI: 10.1177/0300060520954722

[journals.sagepub.com/home/imr](http://journals.sagepub.com/home/imr)



Junyi Hong\*, Fusheng Ye\*, Binjia Yu,  
Junwei Gao, Feicheng Qi\* and Wei Wang\* 

## Abstract

**Objective:** Osteoporosis and osteoarthritis are metabolic skeletal disorders. This study aimed to identify specific networks of competitive endogenous RNA (ceRNA) in osteoporosis that differ from those in osteoarthritis.

**Methods:** The dataset GSE74209 was downloaded from the Gene Expression Omnibus, and differentially expressed microRNAs (DEmiRNAs) in osteoporotic samples and osteoarthritic samples were identified. After predicting target genes and linked long noncoding (lnc)RNAs, ceRNA networks of DEmiRNAs were constructed. The nodes that overlapped between ceRNA networks and the Comparative Toxicogenomics Database were selected as key candidates.

**Results:** Fifteen DEmiRNAs (including 2 downregulated and 13 upregulated miRNAs) were identified in osteoporotic samples versus osteoarthritic samples; these targeted 161 genes and linked to 60 lncRNAs. The ceRNA network consisted of 6 DEmiRNAs, 63 target genes, and 53 lncRNAs. After searching the Comparative Toxicogenomics Database and mining the literature, 2 lncRNAs (*MALAT1* and *NEAT1*), 2 DEmiRNAs (*hsa-miR-32-3p*, downregulated; and *hsa-miR-22-3p*, upregulated) and 6 genes (*SPI1*, *PTEN*, *ESR1*, *ERBB3*, *CSF1R*, and *CDK6*) that relate to cell death, growth, and differentiation were identified as key candidates separating osteoporosis from osteoarthritis.

**Conclusions:** Two miRNA–ceRNA networks (including *NEAT1/MALAT1-hsa-miR-32-3p-SPI1/FZD6* and *NEAT1/MALAT1-hsa-miR-22-3p-PTEN/ESR1/ERBB3/CSF1R/CDK6*) might have crucial and specific roles in osteoporosis.

\*These authors contributed equally to this work.

## Corresponding author:

Wei Wang, Orthopaedics, Zhejiang Xiaoshan Hospital,  
728 Yucai North Road, Xiaoshan District, Hangzhou City,  
Zhejiang Province 311200, China.

Email: [Weiwang19830614@163.com](mailto:Weiwang19830614@163.com)

Department of Orthopaedics, Zhejiang Xiaoshan  
Hospital, Hangzhou City, Zhejiang Province, China



Creative Commons Non Commercial CC BY-NC: This article is distributed under the terms of the Creative

Commons Attribution-NonCommercial 4.0 License (<https://creativecommons.org/licenses/by-nc/4.0/>) which permits non-commercial use, reproduction and distribution of the work without further permission provided the original work is attributed as specified on the SAGE and Open Access pages (<https://us.sagepub.com/en-us/nam/open-access-at-sage>).

## Keywords

Osteoarthritis, Wnt/ $\beta$ -catenin pathway, competitive endogenous RNA, interleukin-6, microRNA, osteoporosis

Date received: 6 April 2020; accepted: 10 August 2020

## Introduction

Osteoporosis and osteoarthritis are metabolic skeletal disorders that are highly prevalent in the older population worldwide.<sup>1</sup> Osteoporosis is more prevalent in postmenopausal women.<sup>1,2</sup> Osteoporosis and osteoarthritis are characterized by compromised bone strength and low bone mass.<sup>3</sup> The prevalence of osteoporosis and the risk of fracture increase with age in women.<sup>4</sup> The risk of fracture is 10% in women at 50 years old, increasing to >20% in women at 80 years old.<sup>4,5</sup> However, the prevalence of fracture risk is relatively stable in men, with a risk lower than 10%.<sup>2,4,5</sup>

Much evidence shows that osteoporosis is correlated with a variety of factors, including age, body mass index, alcohol abuse, smoking, drugs, and increased levels of metabolic and inflammatory markers, such as alkaline phosphatase and adiponectin, among others.<sup>5-10</sup> In particular, obesity, metabolic syndrome, and inflammation are interconnected in the pathogenetic mechanisms underlying osteoporosis.<sup>6-8,10</sup> The levels of inflammatory cytokines, including tumor necrosis factor- $\alpha$  (TNF- $\alpha$ ) and interleukin (IL)-6, are elevated in patients with osteoporosis as well as osteoarthritis.<sup>10-13</sup> Elevated inflammatory status is the cardinal symptom of osteoarthritis.<sup>11</sup>

TNF- $\alpha$  stimulates proinflammatory factors that promote osteoclastogenesis. The causality of TNF- $\alpha$  on osteoclastogenesis is related to the osteoprotegerin/RANKL-ligand/receptor activator of nuclear

factor- $\kappa$ B (OPG/RANKL/RANK) system, which mediates bone resorption.<sup>14,15</sup> OPG binds to RANKLs to block the RANKL/RANK complex and inhibits the activation of downstream nuclear factor- $\kappa$ B (NF- $\kappa$ B) and mitogen-activated protein kinase (MAPK) signaling that contribute to osteoclastogenesis and bone resorption.<sup>14-16</sup> Giner et al.<sup>17</sup> reported that patients with osteoporosis had higher levels of OPG protein compared with patients with osteoarthritis. They also found that 1,25-dihydroxyvitamin D therapy resulted in higher RANKL expression and RANKL:OPG expression ratio in osteoporotic patients than in osteoarthritic patients. These studies suggest a difference in osteoclastogenesis between osteoporosis and osteoarthritis.

Several studies have shown that RANKL-dependent osteoclastogenesis is unnecessary for TNF- $\alpha$ -induced osteoclast differentiation and bone destruction.<sup>18-20</sup> Additionally, numerous studies have shown the involvement of noncoding RNAs, including long noncoding (lnc) RNAs and microRNAs (miRNAs), and signaling (like Wnt/ $\beta$ -catenin pathway) in osteoclastogenesis via either RANKL-dependent or RANKL-independent processes.<sup>21-26</sup> The Wnt/ $\beta$ -catenin pathway is involved in the pathogenesis of both osteoporosis and osteoarthritis.<sup>27-29</sup> The mechanism underlying the pathogenesis of osteoporosis is still unclear, although the identification of genetic factors is helping to elucidate the mechanisms and pathways.

Additionally, systematic differences between osteoporosis and osteoarthritis have not been clearly delineated.

To further clarify the differences in osteoporosis and osteoarthritis, we performed a bioinformatics analysis and identified miRNAs that were differentially expressed in osteoporosis compared with osteoarthritis. The target genes, lncRNAs, and competitive endogenous RNAs (ceRNAs) of the miRNAs were screened out step by step. On the basis of these bioinformatics analyses, we discuss the different mechanisms involved in the pathogenesis of osteoporosis and osteoarthritis.

## Materials and methods

### Microarray data

*Homo sapiens* osteoporosis dataset GSE74209 (GPL20999, miRCURY LNA microRNA Array, 7th generation, hsa, miRBase 20) was downloaded from the National Center of Biotechnology Information Gene Expression Omnibus (GEO; <https://www.ncbi.nlm.nih.gov/geo/>). GSE74209 is composed of 12 samples of fresh femoral neck trabecular bone. These samples were isolated from postmenopausal women who underwent hip replacement due to osteoporotic fracture ( $n = 6$ ) and osteoarthritis ( $n = 6$ ).<sup>30</sup> De-Ugarte et al.<sup>30</sup> obtained ethical approval for obtaining fresh bone samples in their institutions and written informed consent from each participant. Because we used only publicly available datasets in the current study, ethical approval and further informed consent were deemed unnecessary.

### Analysis of differentially expressed miRNAs

The normalized data file (xlsx format, LOcally Weighted Scatterplot Smoothing global regression algorithm) was downloaded. The differentially expressed

miRNAs (DEmiRNAs) between osteoporotic samples and contrast (osteoarthritis) samples were identified using GEO2R in the Limma package (version 3.34.0; <https://bioconductor.org/packages/release/bioc/html/limma.html>). The DEmiRNAs were screened with the criteria of false discovery rate (FDR)  $< 0.05$  and  $|\log_2(\text{FC})| \geq 2$ , where FC is fold change. A heatmap of expression profiles of DEmiRNAs was created using pheatmap (<https://cran.r-project.org/package=pheatmap>).<sup>31</sup>

### Target prediction of DEmiRNAs

Target genes for the DEmiRNAs between osteoporotic and contrast samples were predicted using three programs: miRDB (<http://mirdb.org>), TargetScan Human (<http://www.targetscan.org>), and miRTarBase (<http://mirtarbase.mbc.nctu.edu.tw>). Overlapping target genes that were simultaneously monitored in the three databases were retained and used for further analysis. The miRNA–target regulatory network was constructed and visualized using Cytoscape (version 3.2.0; <http://www.cytoscape.org/>).<sup>32</sup>

### Enrichment analysis for targets

Functional enrichment analysis for the predicted target genes of DEmiRNAs was performed using an R package clusterProfiler (<https://github.com/GuangchuangYu/clusterProfiler>).<sup>33</sup> Gene Ontology (GO) biological process (BP) and the Kyoto Encyclopedia of Genes and Genomes (KEGG) pathways associated with target mRNAs were annotated. Significantly enriched items were screened using the criterion of adjusted  $p$ -value  $< 0.05$ .

### Prediction of miRNA–lncRNA pairs and construction of ceRNA network

To investigate the lncRNAs that may function in osteoporosis, lncRNAs related to the identified DEmiRNAs were screened

using the DIANA Tools webserver (mirPath version 3; <http://snf-515788.vm.okeanos.grnet.gr/>).<sup>34</sup> Accordingly, a ceRNA network of the DE miRNAs in osteoporosis was constructed using Cytoscape.

### Selection of key candidates related to osteoporosis

Before determining the key candidates in osteoporosis, osteoporosis-associated genes, miRNAs, and KEGG pathways were identified in the Comparative Toxicogenomics Database (CTD, 2019 update; <http://ctd.mdibl.org/>) using the search keyword “osteoporosis.” The overlapping items between those identified above and in CTD were regarded as key candidates. GeneCLIP2.0 (<http://ci.smu.edu.cn/>) was further used to mine the literature for evidence on key candidates in osteoporosis.

## Results

### Summary of DE miRNAs

On the basis of the criteria of  $FDR < 0.05$  and  $|\log_2FC| \geq 2$ , 15 DE miRNAs were identified between osteoporotic and osteoarthritic samples of fresh femoral neck trabecular bone. The expression profiles of these DE miRNAs are presented in Figure 1. Two DE miRNAs, *hsa-miR-491-3p* and *hsa-miR-32-3p*, were downregulated in osteoporotic samples compared with osteoarthritic samples, whereas the other 13 DE miRNAs, *ebv-miR-BART6-3p*, *hsa-miR-22-3p*, *hsa-miR-486-5p*, *hsa-miR-3202*, *hsa-miR-4317*, *hsa-miR-675-5p*, *hsa-miR-4306*, *hsa-miR-99a-5p*, *hsa-miR-642a-3p*, *hsa-miR-4687-3p*, *hsa-miR-4534*, *hsa-miR-3158-5p*, and *hsa-miR-4449* were upregulated in osteoporotic samples compared with osteoarthritic samples (Figure 1).

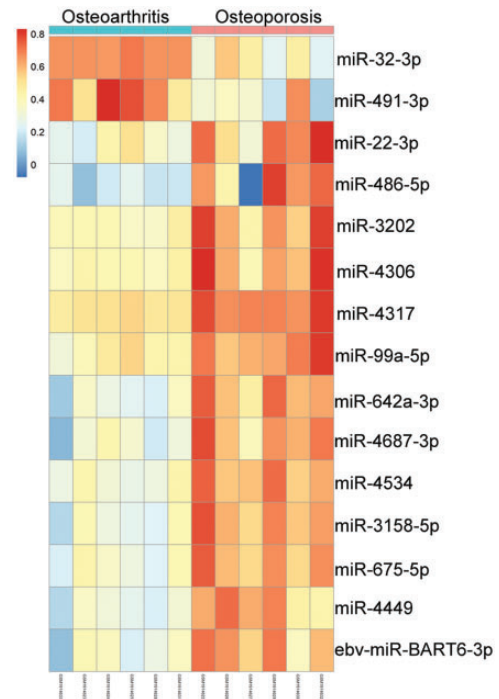


**Figure 1.** Heatmap illustrating expression profiles of differentially expressed microRNAs (miRNAs) in osteoarthritis and osteoporosis. Red and blue colors indicate high and low expression of miRNA, respectively.

### miRNA–target network of target genes

A total of 161 target genes of 11 DE miRNAs were identified from miRDB, TargetScanHuman, and miRTarBase. The count of target genes for each DE miRNA ranged from 1 to 46. The resulting miRNA–target network consisted of 11 miRNAs, 161 genes, and 163 interactions (Figure 2). Of the miRNAs, *hsa-miR-22-3p*, *hsa-miR-3202*, *hsa-miR-32-3p*, and *hsa-miR-4534* miRNAs regulated the greatest number of genes, with 32, 46, 14, and 30 target genes, respectively.

### Enrichment analysis of target genes

To determine the biological functions of the miRNAs, we performed functional

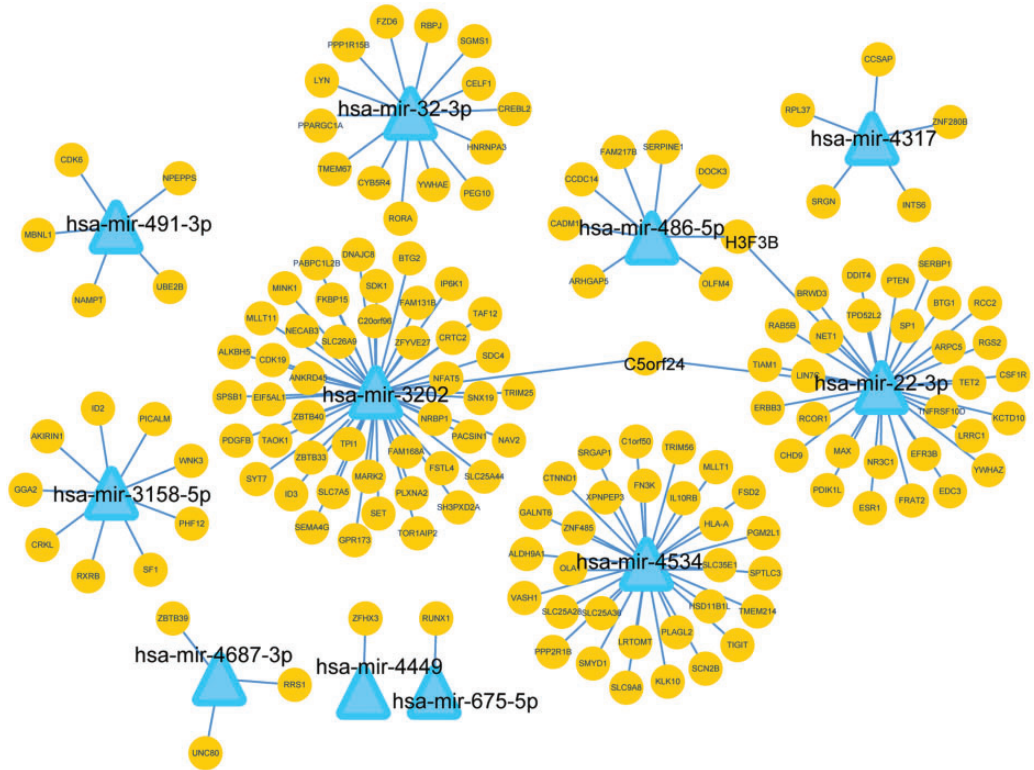


**Figure 2.** The microRNA (miRNA)–target regulatory network. Triangles and circles represent miRNA and target genes, respectively.

enrichment analysis of their target genes. Enrichment analysis indicated that functional BP such as “locomotor rhythm” (GO: 0045475), “myoblast differentiation” (GO: 0045445), “muscle cell proliferation” (GO: 0033002), and “myeloid leukocyte differentiation” (GO: 0002573) involved target genes including cyclin-dependent kinase 6 (*CDK6*), mechanistic target of rapamycin kinase (mTOR), serpin family E member 1 (*SERPINE1*), nicotinamide phosphoribosyltransferase (*NAMPT*), phosphatase and tensin homolog (*PTEN*), recombination signal binding protein for immunoglobulin kappa J (*RBPJ*), peroxisome proliferator-activated receptor- $\gamma$  coactivator 1 $\alpha$  (*PPARGC1A*), erb-b2 receptor tyrosine kinase 3 (*ERBB3*), and regulator of G protein signaling 2 (*RGS2*; Table 1).

The KEGG pathways “PI3K-Akt signaling pathway” (hsa04151), “EGFR tyrosine kinase inhibitor resistance” (hsa01521), “Hippo signaling pathway” (hsa04390), and “Rap1 signaling pathway” (hsa04015) enriched target genes such as colony-stimulating factor 1 receptor (*CSF1R*), *ERBB3*, *CDK6*, *PTEN*, and DNA damage inducible transcript 4 (*DDIT4*), *mTOR*, and frizzled class receptor 6 (*FZD6*; Table 1).

### Construction of ceRNA network

Before we constructed the ceRNA network, the lncRNAs related to the 11 DE miRNAs in the miRNA–target network were screened using DIANA Tools. Sixty lncRNAs that regulated six DE miRNAs were screened. The ceRNA network, which consisted of 6

**Table 1.** Results of the GO and KEGG functional enrichment analysis for the target genes of differentially expressed miRNAs.

ID	Description	No.	p-value	Adjusted p-value	Gene symbol
<i>Biological process (significant)</i>					
GO: 0045475	Locomotor rhythm	4	$5.84 \times 10^{-6}$	0.017	MTOR, ID2, PTEN, ZFHX3
GO: 0006367	Transcription initiation from RNA polymerase II promoter	9	$1.83 \times 10^{-5}$	0.024	RBPI, NRBPI, RORA, RXRB, ESRI, NR3C1, TAF12, PTEN, PPARGC1A
GO: 0006352	DNA-templated transcription, initiation	10	$2.39 \times 10^{-5}$	0.024	RBPI, NRBPI, RORA, RXRB, ESRI, NR3C1, TAF12, PTEN, SMARCA5, PPARGC1A
GO: 0007569	Cell aging	7	$5.23 \times 10^{-5}$	0.033	CDK6, MTOR, SERPINE1, VASH1, ID2, NAMPT, PTEN
GO: 0045445	Myoblast differentiation	6	$6.23 \times 10^{-5}$	0.033	AKIRIN1, RBPI, BTG1, MBNL1, ID3, SMYD1
GO: 0046777	Protein autophosphorylation	9	$6.67 \times 10^{-5}$	0.033	MTOR, FGF3, LYN, WNK3, MARK2, MINK1, TAOK1, PDGFB, CSF1R
GO: 0016358	Dendrite development	9	$8.28 \times 10^{-5}$	0.035	TIAMI, MTOR, PICALM, FSTL4, CRKL, MINK1, PTEN, PACSINI, SDKI
GO: 0019216	Regulation of lipid metabolic process	12	$1.38 \times 10^{-4}$	0.042	RORA, MTMR3, MTOR, SPI, FGFR3, LYN, ID2, CHD9, SFI, PDGFB, CREBL2, PPARGC1A
GO: 0048511	Rhythmic process	10	$1.47 \times 10^{-4}$	0.042	RORA, MTOR, ESRI, SPI, SERPINE1, ID2, NAMPT, PTEN, ZFHX3, PPARGC1A
GO: 0032922	Circadian regulation of gene expression	5	$1.52 \times 10^{-4}$	0.042	RORA, ID2, NAMPT, ZFHX3, PPARGC1A
GO: 0050773	Regulation of dendrite development	7	$1.63 \times 10^{-4}$	0.042	TIAMI, MTOR, FSTL4, CRKL, PTEN, PACSINI, SDKI
GO: 0001933	Negative regulation of protein phosphorylation	12	$1.90 \times 10^{-4}$	0.042	PPP1R15B, UBE2B, RGS2, MTOR, TRIB2, MLLT1, LYN, CTDSP1, CRKL, DDIT4, PTEN, PPARGC1A
GO: 0033002	Muscle cell proliferation	9	$2.02 \times 10^{-4}$	0.042	AKIRIN1, RBPI, MTOR, ID2, NAMPT, SFI, PTEN, PDGFB, PPARGC1A
GO: 0014812	Muscle cell migration	6	$2.21 \times 10^{-4}$	0.042	AKIRIN1, SERPINE1, ARPC5, PDGFB, PPARGC1A, NET1
GO: 0021542	Dentate gyrus development	3	$2.38 \times 10^{-4}$	0.042	CDK6, BTG2, PTEN
GO: 0021761	Limbic system development	6	$2.58 \times 10^{-4}$	0.042	CDK6, YWHAE, BTG2, CRKL, ARPC5, PTEN
GO: 0002573	Myeloid leukocyte differentiation	8	$2.82 \times 10^{-4}$	0.042	AKIRIN1, RBPI, MTOR, ID2, NAMPT, SFI, PTEN, PDGFB, PPARGC1A

(continued)

**Table 1.** Continued.

ID	Description	No.	p-value	Adjusted p-value	Gene symbol
GO: 0007623	Circadian rhythm	8	$2.82 \times 10^{-4}$	0.042	RORA, MTOR, SERPINE1, ID2, NAMPT, PTEN, ZFHx3, PPARGC1A
GO: 0010810	Regulation of cell-substrate adhesion	8	$2.82 \times 10^{-4}$	0.042	CDK6, OLFM4, SERPINE1, RCC2, CRKL, SDC4, MINK1, PTEN
GO: 1901861	Regulation of muscle tissue development	7	$2.83 \times 10^{-4}$	0.042	AKIRIN1, RBPJ, ERBB3, RGS2, MTOR, PTEN, PPARGC1A
GO: 0060998	Regulation of dendritic spine development	5	$3.12 \times 10^{-4}$	0.044	TIAMI, MTOR, FSTL4, PTEN, SDKI
KEGG pathways (top 15)					
hsa04151	PI3K-Akt signaling pathway	12	$7.98 \times 10^{-5}$	0.014	CDK6, ERBB3, MTOR, YWHAE, FGFR3, PPP2R1B, YWHAZ, DDIT4, PTEN, PDGFB, CSF1R, CRTCL
hsa05202	Transcriptional misregulation in cancer	8	$2.84 \times 10^{-4}$	0.022	RUNX1, RXRB, H3F3B, SPI, MLLT1, ID2, MAX, CSF1R
hsa05224	Breast cancer	7	$3.77 \times 10^{-4}$	0.022	CDK6, FRAT2, MTOR, ESRI, SPI, FZD6, PTEN
hsa01521	EGFR tyrosine kinase inhibitor resistance	5	$7.57 \times 10^{-4}$	0.033	ERBB3, MTOR, FGFR3, PTEN, PDGFB
hsa04390	Hippo signaling pathway	6	$2.81 \times 10^{-3}$	0.097	YWHAE, SERPINE1, PPP2R1B, ID2, FZD6, YWHAZ
hsa05230	Central carbon metabolism in cancer	4	$3.61 \times 10^{-3}$	0.105	MTOR, FGFR3, SLC7A5, PTEN
hsa05214	Glioma	4	$4.87 \times 10^{-3}$	0.121	CDK6, MTOR, PTEN, PDGFB
hsa03018	RNA degradation	4	$5.86 \times 10^{-3}$	0.127	BTG1, BTG2, EDC3, PABPC1L2B
hsa05206	MicroRNAs in cancer	8	$7.26 \times 10^{-3}$	0.135	CDK6, ERBB3, MTOR, FGFR3, CRKL, DDIT4, PTEN, PDGFB
hsa04550	Signaling pathways regulating pluripotency of stem cells	5	$9.10 \times 10^{-3}$	0.135	FGFR3, ID3, ID2, FZD6, ZFHx3
hsa05222	Small cell lung cancer	4	$9.97 \times 10^{-3}$	0.135	CDK6, RXRB, MAX, PTEN
hsa05203	Viral carcinogenesis	6	$1.01 \times 10^{-2}$	0.135	RBPJ, CDK6, YWHAE, LYN, HLA-A, YWHAZ
hsa04350	TGF-beta signaling pathway	4	$1.07 \times 10^{-2}$	0.135	SPI, PPP2R1B, ID3, ID2
hsa05205	Proteoglycans in cancer	6	$1.09 \times 10^{-2}$	0.135	TIAMI, ERBB3, MTOR, ESRI, FZD6, SDC4
hsa04015	Rap1 signaling pathway	6	$1.24 \times 10^{-2}$	0.142	TIAMI, FGFR3, CRKL, PDGFB, CSF1R, CTNND1

miRNA, microRNA; GO, Gene Ontology; KEGG, Kyoto Encyclopedia of Genes and Genomes.

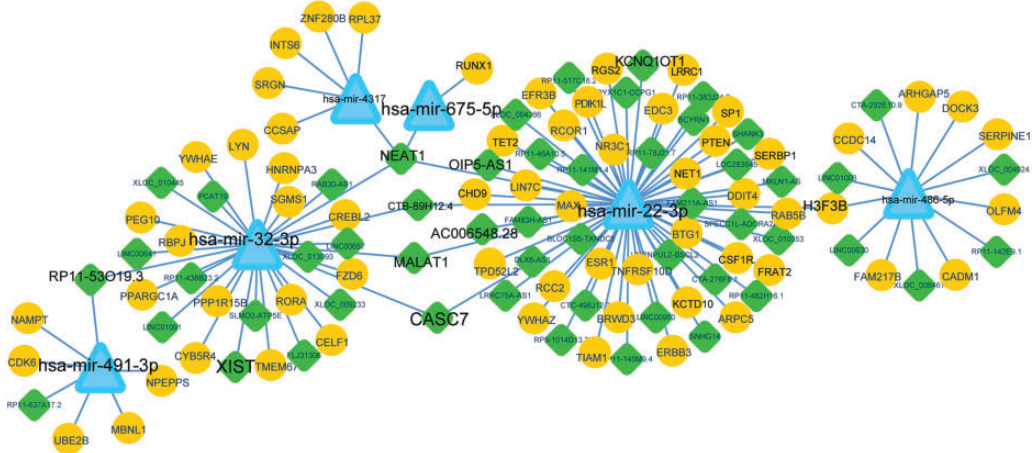


**Figure 3.** Competing endogenous RNA (ceRNA) network in osteoporosis. Diamonds, triangles, and circles indicate long noncoding (lnc)RNA, microRNA (miRNA), and target genes, respectively. The key candidates are shown in a larger font.

DEmiRNAs, 63 target genes, and 53 lncRNAs, was constructed accordingly (Figure 3). LncRNAs, including nuclear paraspeckle assembly transcript 1 (*NEAT1*), metastasis-associated lung adenocarcinoma transcript 1 (*MALAT1*), cancer susceptibility candidate 7 (*CASC7*), *RP11-53019.3*, and *CTB-89H12.4*, regulated more than 2 miRNAs, including *hsa-miR-22-3p*, *hsa-miR-675-5p*, *hsa-miR-32-3p*, and *hsa-miR-491-3p*. In addition, *hsa-miR-22-3p* and *hsa-miR-32-3p* were regulated by 33 and 17 lncRNAs, respectively. The count of target genes of *hsa-miR-22-3p*, *hsa-miR-32-3p*, *hsa-miR-486-5p*, and *hsa-miR-491-3p* was 30, 14, 8, and 5, respectively.

### Selection of key candidates related to osteoporosis

The genes and pathways associated with “osteoporosis” and “osteoporosis, postmenopausal” were downloaded from CTD. Seven lncRNAs (*AC006548.28*, *MALAT1*, *XIST*, *NEAT1*, *RP11-53019.3*, *KCNQ10T1*, and *OIP5-AS1*), 4 miRNAs (*hsa-miR-22*, *hsa-miR-32*, *hsa-miR-491*, and *hsa-miR-675*), and 63 target genes

(including *CSF1R*, *SPI*, *ERBB3*, *CDK6*, *PTEN*, *SERPINE1*, and *FZD6*; Table 2) overlapped in CTD. Finally, 13 genes that enriched significant pathways (adjusted  $p < 0.05$ ) were selected as key genes. However, none of the target genes were enriched in the KEGG pathways retrieved from CTD (Table 3). *IL6* and IL-6 receptor (*IL6R*) were hub genes related to osteoporosis in CTD, whereas *ESR1*, *SPI*, *CSF1R*, *ERBB3*, *CDK6*, and *PTEN* were hub genes identified in our study. The Wnt signaling factor *Wnt1* and *FZD6* were enriched in breast cancer (Table 3).

Finally, we submitted the 13 genes, 4 miRNAs, and 7 lncRNAs to GeneCLiP2.0 and obtained a heatmap of “gene cluster with literature profiles” using criteria of hit  $\geq 8$ , enrichment score  $\geq 5.0$ , and  $p < 1e-04$  (Figure 4). We observed that *SPI*, *PTEN*, *ESR1*, *ERBB3*, *CSF1R*, and *CDK6* were associated with cell growth, cell death, signaling transducer, estrogen receptor, histone deacetylase inhibitor, and several types of human cancers, such as breast cancer and squamous cell carcinoma (Figure 4). DEmiRNAs *hsa-miR-22* and



**Table 2.** Key candidates in osteoporosis that overlapped in the Comparative Toxicogenomics Database.

lncRNA/miRNA	Gene	Gene	Gene
<i>AC006548.28</i>	<i>KCTD10</i>	<i>DDIT4</i>	<i>YWHAE</i>
<i>MALAT1</i>	<i>LIN7C</i>	<i>DOCK3</i>	<i>YWHAZ</i>
<i>XIST</i>	<i>NPEPPS</i>	<i>EDC3</i>	<i>BRWD3</i>
<i>NEAT1</i>	<i>RPL37</i>	<i>EFR3B</i>	<i>RUNX1</i>
<i>RP11-53019.3</i>	<i>SERBP1</i>	<i>ERBB3</i>	<i>FAM217B</i>
<i>KCNQ1OT1</i>	<i>TET2</i>	<i>ESR1</i>	<i>HNRNPA3</i>
<i>OIP5-AS1</i>	<i>TPD52L2</i>	<i>FRAT2</i>	<i>INTS6</i>
<i>hsa-miR-22</i>	<i>UBE2B</i>	<i>FZD6</i>	<i>LRRC1</i>
<i>hsa-miR-32</i>	<i>ZNF280B</i>	<i>H3F3B</i>	<i>LYN</i>
<i>hsa-miR-491</i>	<i>PPARGC1A</i>	<i>RGS2</i>	<i>MAX</i>
<i>hsa-miR-675</i>	<i>ARHGAP5</i>	<i>RORA</i>	<i>MBNL1</i>
	<i>ARPC5</i>	<i>SERPINE1</i>	<i>NAMPT</i>
	<i>BTG1</i>	<i>SGMS1</i>	<i>NET1</i>
	<i>CADM1</i>	<i>SHANK3</i>	<i>NR3C1</i>
	<i>CCDC14</i>	<i>SPI</i>	<i>OLFM4</i>
	<i>CCSAP</i>	<i>SRGN</i>	<i>PDIK1L</i>
	<i>CDK6</i>	<i>TIAM1</i>	<i>PEG10</i>
	<i>CHD9</i>	<i>TMEM67</i>	<i>PPP1R15B</i>
	<i>CSF1R</i>	<i>TNFRSF10D</i>	<i>PTEN</i>
	<i>CREBL2</i>	<i>RAB5B</i>	<i>RCC2</i>
	<i>CY5R4</i>	<i>RBPJ</i>	<i>UBE2B</i>

lncRNA, long noncoding RNA; miRNA, microRNA.

**Table 3.** Key Kyoto Encyclopedia of Genes and Genomes pathways and related genes retrieved from the CTD.

ID	Description	Gene symbol	Adjusted p-value	Gene in CTD
hsa04151*	PI3K-Akt signaling pathway	<i>CDK6, ERBB3, YWHAE, YWHAZ, DDIT4, PTEN, CSF1R</i>	0.014	<i>COL1A1, COL1A2, IL6, IL6R</i>
hsa05202*	Transcriptional misregulation in cancer	<i>RUNX1, RXRB, H3F3B, SPI, MAX, CSF1R</i>	0.022	<i>IL6</i>
hsa05224*	Breast cancer	<i>CDK6, FRAT2, ESR1, SPI, FZD6, PTEN</i>	0.022	<i>LRP5, TNFSF11, WNT1</i>
hsa01521*	EGFR tyrosine kinase inhibitor resistance	<i>ERBB3, PTEN</i>	0.033	<i>IL6, IL6R</i>

CTD, Comparative Toxicogenomics Database.

\*Adjusted  $p < 0.05$ .

*hsa-miR-32* were associated with cell growth, differentiation, or apoptosis, and the lncRNA *NEAT1* and *MALAT1* were related to cell death/growth and human

cancers. These results indicated that the ceRNA axes *NEAT1/MALAT1-hsa-miR-32-3p-SPI/FZD6* and *NEAT1/MALAT1-hsa-miR-22-3p-PTEN/ESR1/ERBB3/CSF1*



**Figure 4.** Functional clustering of key candidates using literature mining. Green and black indicate that the corresponding gene-term association was positively and negatively reported, respectively. Criteria were hit  $\geq 8$ , enrichment score  $>5.0$  and  $p < 1e-04$ .

*R/CDK6* might have important roles in osteoporosis.

**Discussion**

Our study identified several genes (e.g., *PTEN*, *ESR1*, *ERBB3*, *RUNX1*, *FZD6*,

*CSF1R*, and *CDK6*), miRNAs (e.g., *hsa-miR-22-3p*, *hsa-miR-675-5p*, and *hsa-miR-32-3p*), and lncRNAs (e.g., *NEAT1* and *MALAT1*) that may have crucial roles in the pathogenesis of osteoporosis. Two ceRNA networks, *NEAT1/MALAT1-hsa-miR-32-3p-SP1/FZD6* and *NEAT1/MALA*

*T1-hsa-miR-22-3p-PTEN/ESR1/ERBB3/CSF1R/CDK6*, were identified. The potential of these networks and factors in osteoporosis support its complex pathogenic mechanism and uncover important clinical–translational implications. These identified biomarkers could, in fact, yield new potential therapeutic targets for osteoporosis.

Inflammation is a contributing factor to the development of postmenopausal osteoporosis.<sup>35,36</sup> Elevated circulating levels of IL-1 $\beta$ , TNF- $\alpha$ , and IL-6 are positively associated with bone destruction, bone loss, and excessive bone resorption.<sup>10,15,16,35,37</sup> The canonical Wnt/ $\beta$ -catenin pathway is an osteoblastic pathway.<sup>24–26</sup> *SPI* is a transcription factor that promotes osteoporosis.<sup>24,38,39</sup> Li et al.<sup>24</sup> reported that *SPI* inhibited the activation of Wnt/ $\beta$ -catenin signaling by stimulating the expression of *miR-545-3p/LRP5*. A polymorphism in the *SP1*-binding site in the collagen I  $\alpha 1$  gene (*COL1A*) is associated with osteoporosis.<sup>38</sup> Moreover, the assembly of *SP1* and *RARB* on the promoter of bone morphogenetic protein 2 (*BMP2*) inactivates the *BMP2* gene.<sup>39</sup>

In the present study, we found that *SPI* was a target of *hsa-miR-32-3p*, whereas Wnt receptor *FZD6* was a target of *hsa-miR-22-3p*. Expression of *hsa-miR-22-3p* and *hsa-miR-32-3p* was upregulated in fresh femoral neck trabecular bone samples obtained from patients with osteoporosis and osteoarthritis, respectively. Thus, we propose probable upregulation of *FZD6*, downregulation of *SPI*, and higher expression of *hsa-miR-32-3p-SPI/FZD6*-mediated Wnt/ $\beta$ -catenin signaling in osteoporosis compared with osteoarthritis. This finding is interesting because Wnt/ $\beta$ -catenin signaling is upregulated in both osteoporosis and osteoarthritis and is even considered a target for their treatment.<sup>24,28,29,40,41</sup> In osteoblasts, the Wnt/ $\beta$ -catenin osteoblastic pathway is inactivated by IL-6,<sup>42</sup> which can

also inhibit the RANKL/RANK signaling pathway.<sup>43</sup> That osteoporotic patients had higher levels of OPG protein than osteoarthritic patients might indicate lower expression of RANKL/RANK signaling pathway in osteoporosis.<sup>17</sup> The upregulation of OPG in osteoporotic patients compared with osteoarthritic patients in our study may provide a sign that the levels of inflammatory cytokines (i.e., TNF- $\alpha$  and IL-6) are lower in osteoporotic patients than in osteoarthritic patients.

The lncRNA *NEAT1* and *MALAT1* are often considered to be tumor-related lncRNAs,<sup>44</sup> but evidence also correlates these lncRNA with osteogenic differentiation.<sup>45–48</sup> Several studies show that *NEAT1* and *MALAT1* promote osteoblast differentiation by sponging miRNAs such as miR-214 and miR-204.<sup>46–48</sup> In contrast, Li et al.<sup>45</sup> showed that silencing *MALAT1* in lipopolysaccharide-treated chondrocytes promoted IL-6 expression and apoptosis by sponging and inactivating miR-146a. Our results revealed that downregulated *hsa-miR-32-3p* and upregulated *hsa-miR-22-3p* were simultaneously regulated by *NEAT1* and *MALAT1*. The correlation of *NEAT1*- and *MALAT1*-mediated networks should be validated using further experiments.

Another cluster of genes that associate with PI3K/Akt signaling pathway, breast cancer, and epidermal growth factor receptor (EGFR) tyrosine kinase inhibitor resistance were targets of the upregulated *hsa-miR-22-3p*, including *PTEN*, *ESR1*, *ERBB3*, *CSF1R*, and *CDK6*. *PTEN* and *ERBB3* have been reported to be linked to pathogenesis, development, and drug resistance in several types of human cancer, including colorectal cancer, breast cancer, and lung cancer,<sup>49,50</sup> but not osteoclastogenesis. PI3K/*PTEN* signaling is essential for embryonic development, angiogenesis, and tumorigenesis. *PTEN* can be regulated by multiple miRNAs, including miR-185

and miR-132.<sup>51,52</sup> miR-132 regulates osteogenic differentiation by targeting Sirtuin1,<sup>53</sup> and miR-185 inhibits osteogenic differentiation by downregulating Wnt/ $\beta$ -catenin signaling.<sup>54</sup> *ESR1* is associated with the concentration of high-density lipoproteins and total fat tissue content.<sup>55</sup> *CSF1R* inhibition suppresses osteoclast formation and prevents lipopolysaccharide-induced osteoporosis.<sup>56</sup> *CDK6* expression was positively correlated with chondrocyte proliferation in osteoarthritic rabbits.<sup>57</sup> We showed here that *PTEN*, *ESR1*, *ERBB3*, *CSF1R*, and *CDK6* were regulated by *NEAT1/MALAT1* by sponging and inhibiting *hsa-miR-22-3p*. These might show a novel and potential mechanism of osteoporosis that is related to the pathology of osteoarthritis.

The PI3K/Akt/mTOR pathway plays a crucial role in cellular growth, proliferation, angiogenesis, tumor immunity, and bone metabolism.<sup>58,59</sup> Its inhibition activates osteoclast proliferation and increases bone mass.<sup>58</sup> 17-Allylamino-17-demethoxygeldanamycin (17-AAG) is a geldanamycin derivative and inhibitor of heat shock protein 90 (Hsp90).<sup>59</sup> 17-AAG-induced inhibition of Hsp90 can enhance bone formation and rescue glucocorticoid-induced bone loss.<sup>60</sup> 17-AAG also induces the inhibition of Akt, mTOR, and glycogen synthase kinase-3 $\beta$  (GSK-3 $\beta$ ), and promotes the apoptosis of osteosarcoma cell lines.<sup>59,61</sup> GSK-3 $\beta$  is a negative regulator of the canonical Wnt/ $\beta$ -catenin signaling.<sup>62</sup> These results might show that 17-AAG is a potential therapeutic target for osteoporosis, and Wnt/ $\beta$ -catenin and PI3K/Akt signaling might be common therapeutic targets in the management of both osteoporosis and osteosarcoma.

## Conclusion

This bioinformatics analysis identified different mechanisms underlying osteoporosis and osteoarthritis. The key targets of

DEmiRNAs between osteoporotic and osteoarthritic samples were osteogenic differentiation or osteoclastogenesis through pathways including PI3K/Akt and Wnt/ $\beta$ -catenin. Wnt/ $\beta$ -catenin signaling may be upregulated in osteoporosis compared with osteoarthritis. Two ceRNA networks, *NEAT1/MALAT1-hsa-miR-32-3p-SP1/FZD6* and *NEAT1/MALAT1-hsa-miR-22-3p-PTEN/ESR1/ERBB3/CSF1R/CDK6*, may have specific and potential roles in osteoporosis.

## Declaration of conflicting interest

The authors declare that there is no conflict of interest.


## Funding

This research received no specific grant from any funding agency in the public, commercial, or not-for-profit sectors.

## Author contributions

JH, FY, and WW conceived and designed the study. FY, BY, and JG were responsible for data acquisition, statistical analysis, and interpretation. JH and FY drafted the manuscript. FQ and WW revised the manuscript for important intellectual content. All authors have read and approved the manuscript.

## ORCID iD

Wei Wang  <https://orcid.org/0000-0002-1839-9422>

## References

1. Ganguly P, El-Jawhari JJ, Giannoudis PV, et al. Age-related changes in bone marrow mesenchymal stromal cells: a potential impact on osteoporosis and osteoarthritis development. *Cell Transplant* 2017; 26: 1520–1529.
2. Miyakoshi N, Kasukawa Y, Hongo M, et al. Prevalence of non-responders to both oral bisphosphonate monotherapy and intravenous ibandronate in patients with

- postmenopausal osteoporosis. *Open J Orthop* 2020; 10: 43.
3. Eastell R, O'Neill TW, Hofbauer LC, et al. Postmenopausal osteoporosis. *Nat Rev Dis Primers* 2016; 2: 16069.
  4. Kaushal N, Vohora D, Jalali RK, et al. Prevalence of osteoporosis and osteopenia in an apparently healthy Indian population-a cross-sectional retrospective study. *Osteoporos Sarcopenia* 2018; 4: 53–60.
  5. Noh JW, Park H, Kim M, et al. Gender differences and socioeconomic factors related to osteoporosis: a cross-sectional analysis of nationally representative data. *J Womens Health (Larchmt)* 2018; 27: 196–202.
  6. Ciccarelli F, De Martinis M and Ginaldi L. Glucocorticoids in patients with rheumatic diseases: friends or enemies of bone? *Curr Med Chem* 2015; 22: 596–603.
  7. Ginaldi L and De Martinis M. Osteoimmunology and beyond. *Curr Med Chem* 2016; 23: 3754–3774.
  8. Lubkowska A, Dobek A, Mieszkowski J, et al. Adiponectin as a biomarker of osteoporosis in postmenopausal women: controversies. *Dis Markers* 2014; 2014: 1–14.
  9. Yoon V, Maalouf NM and Sakhaee K. The effects of smoking on bone metabolism. *Osteoporos Int* 2012; 23: 2081–2092.
  10. Migliaccio S, Greco EA, Fornari R, et al. Is obesity in women protective against osteoporosis? *Diabetes Metab Syndr Obes* 2011; 4: 273–282.
  11. Brennan FM, McInnes IB, Brennan FM, et al. Evidence that cytokines play a role in rheumatoid arthritis. *J Clin Invest* 2008; 118: 3537–3545.
  12. Taguchi Y, Yamamoto M, Yamate T, et al. Interleukin-6-type cytokines stimulate mesenchymal progenitor differentiation toward the osteoblastic lineage. *Proc Assoc Am Physicians* 1998; 110: 559–574.
  13. Dodds RA, Merry K, Littlewood A, et al. Expression of mRNA for IL1 beta, IL6 and TGF beta 1 in developing human bone and cartilage. *J Histochem Cytochem* 1994; 42: 733–744.
  14. Chen G, Xu Q, Dai M, et al. Bergapten suppresses RANKL-induced osteoclastogenesis and ovariectomy-induced osteoporosis via suppression of NF- $\kappa$ B and JNK signaling pathways. *Biochem Biophys Res Commun* 2019; 509: 329–334.
  15. Oliveira MC, Vullings J and Van De Loo FAJ. Osteoporosis and osteoarthritis are two sides of the same coin paid for obesity. *Nutrition* 2019; 70: 110486.
  16. Tanaka S. RANKL-independent osteoclastogenesis: a long-standing controversy. *J Bone Miner Res* 2017; 32: 431–433.
  17. Giner M, Rios MJ, Montoya MJ, et al. RANKL/OPG in primary cultures of osteoblasts from post-menopausal women. Differences between osteoporotic hip fractures and osteoarthritis. *J Steroid Biochem Mol Biol* 2009; 113: 46–51.
  18. Lam J, Takeshita S, Barker JE, et al. TNF- $\alpha$  induces osteoclastogenesis by direct stimulation of macrophages exposed to permissive levels of RANK ligand. *J Clin Invest* 2000; 106: 1481–1488.
  19. Kim N. Osteoclast differentiation independent of the TRANCE-RANK-TRAF6 axis. *J Exp Med* 2005; 202: 589–595.
  20. Feng W, Guo J and Li M. RANKL-independent modulation of osteoclastogenesis. *J Oral Biosci* 2019; 61: 16–21.
  21. Che W, Dong Y and Quan HB. RANKL inhibits cell proliferation by regulating MALAT1 expression in a human osteoblastic cell line hFOB 1.19. *Cell Mol Biol (Noisy-le-grand)* 2015; 61: 7–14.
  22. Yongyun C, Degang Y, Wenxiang C, et al. LncRNA expression profiles and the negative regulation of lncRNA-NOMMUT037835.2 in osteoclastogenesis. *Bone* 2020; 130: 8756–3282.
  23. Xu Z, Liu X, Wang H, et al. Lung adenocarcinoma cell-derived exosomal miR-21 facilitates osteoclastogenesis. *Gene* 2018; 666: 116–122.
  24. Li L, Qiu X, Sun Y, et al. SP1-stimulated miR-545-3p inhibits osteogenesis via targeting LRP5-activated Wnt/ $\beta$ -catenin signaling. *Biochem Biophys Res Commun* 2019; 517: 103–110.
  25. Zhang ND, Han T, Huang BK, et al. Traditional Chinese medicine formulas for the treatment of osteoporosis: implication for antiosteoporotic drug discovery. *J Ethnopharmacol* 2016; 189: 61–80.

26. Molagoda IMN, Karunarathne WAHM, Choi YH, et al. Fermented oyster extract promotes osteoblast differentiation by activating the Wnt/ $\beta$ -catenin signaling pathway, leading to bone formation. *Biomolecules* 2019; 9: 711.
27. Xi Y, Huang X, Tan G, et al. Protective effects of Erdosteine on interleukin-1 $\beta$ -stimulated inflammation via inhibiting the activation of MAPK, NF- $\kappa$ B, and Wnt/ $\beta$ -catenin signaling pathways in rat osteoarthritis. *Eur J Pharmacol* 2020; 873: 172925.
28. Deshmukh V, O'Green AL, Bossard C, et al. Modulation of the Wnt pathway through inhibition of CLK2 and DYRK1A by lorecivint as a novel, potentially disease-modifying approach for knee osteoarthritis treatment. *Osteoarthritis Cartilage* 2019; 27: 1347–1360.
29. Stampella A, Monteagudo S and Lories R. Wnt signaling as target for the treatment of osteoarthritis. *Best Pract Res Clin Rheumatol* 2017; 31: 721–729.
30. De-Ugarte L, Yoskovitz G, Balcells S, et al. MiRNA profiling of whole trabecular bone: identification of osteoporosis-related changes in MiRNAs in human hip bones. *BMC Med Genomics* 2016; 8: 75.
31. Szekely GJ and Rizzo ML. Hierarchical clustering via joint between-within distances: Extending Ward's minimum variance method. *J Classif* 2005; 22: 151–183.
32. Shannon P, Markiel A, Ozier O, et al. Cytoscape: a software environment for integrated models of biomolecular interaction networks. *Genome Res* 2003; 13: 2498–2504.
33. Yu G, Wang LG, Han Y, et al. clusterProfiler: an R package for comparing biological themes among gene clusters. *OMICS* 2012; 16: 284–287.
34. Vlachos IS and Hatzigeorgiou AG. Functional analysis of miRNAs using the DIANA Tools online suite. *Drug Target miRNA*. Springer, 2017. pp.25–50.
35. Al-Daghri NM, Aziz I, Yakout S, et al. Inflammation as a contributing factor among postmenopausal Saudi women with osteoporosis. *Medicine (Baltimore)* 2017; 96: e5780. doi: 10.1097/MD.0000000000005780.
36. Ji YF, Jiang X, Li W, et al. Impact of interleukin-6 gene polymorphisms and its interaction with obesity on osteoporosis risk in Chinese postmenopausal women. *Environ Health Prev Med* 2019; 24: 48.
37. Yokota K. Inflammation and osteoclasts. *Japanese Journal of Clinical Immunology* 2017; 40: 367–376.
38. Kurt-Sirin O, Yilmaz-Aydogan H, Uyar M, et al. Combined effects of collagen type I alpha1 (COL1A1) Sp1 polymorphism and osteoporosis risk factors on bone mineral density in Turkish postmenopausal women. *Gene* 2014; 540: 226–231. doi: 10.1016/j.gene.2014.02.028
39. Xu J and Rogers MB. Modulation of bone morphogenetic protein (BMP) 2 gene expression by Sp1 transcription factors. *Gene* 2007; 392: 221–229.
40. Baron R and Gori F. Targeting WNT signaling in the treatment of osteoporosis. *Curr Opin Pharmacol* 2018; 40: 134–141.
41. De Martinis M, Sirufo MM and Ginaldi L. Osteoporosis: current and emerging therapies targeted to immunological checkpoints. *Curr Med Chem* 2020. doi: 10.2174/0929867326666190730113123.
42. Malysheva K, Rooij KD, WGM Löwik C, et al. Interleukin 6/Wnt interactions in rheumatoid arthritis: interleukin 6 inhibits Wnt signaling in synovial fibroblasts and osteoblasts. *Croat Med J* 2016; 57: 89–98.
43. Kim B, Lee KY and Park B. Icaritin abrogates osteoclast formation through the regulation of the RANKL-mediated TRAF6/NF- $\kappa$ B/ERK signaling pathway in Raw264.7 cells. *Phytomedicine* 2018; 51: 181–190.
44. Arshi A, Sharifi FS, Khorramian Ghahfarokhi M, et al. Expression analysis of MALAT1, GAS5, SRA, and NEAT1 lncRNAs in breast cancer tissues from young women and women over 45 years of age. *Mol Ther Nucleic Acids* 2018; 12: 751–757.
45. Li H, Xie S, Li H, et al. LncRNA MALAT1 mediates proliferation of LPS treated-articular chondrocytes by targeting the miR-146a-PI3K/Akt/mTOR axis. *Life Sci* 2019; 116801.

46. Zhang Y, Chen B, Li D, et al. LncRNA NEAT1/miR-29b-3p/BMP1 axis promotes osteogenic differentiation in human bone marrow-derived mesenchymal stem cells. *Pathol Res Pract* 2019; 215: 525–531.
47. Xiao X, Zhou T, Guo S, et al. LncRNA MALAT1 sponges miR-204 to promote osteoblast differentiation of human aortic valve interstitial cells through up-regulating Smad4. *Int J Cardiol Heart Vasc* 2017; 243: 404–412.
48. Huang XZ, Huang J, Li WZ, et al. LncRNA-MALAT1 promotes osteogenic differentiation through regulating ATF4 by sponging miR-214: implication of steroid-induced avascular necrosis of the femoral head. *Steroids* 2020; 154: 108533.
49. Cao L, Basudan A, Sikora MJ, et al. Frequent amplifications of ESR1, ERBB2 and MDM4 in primary invasive lobular breast carcinoma. *Cancer Lett* 2019; 461: 21–30.
50. Ross JS, Fakhri M, Ali SM, et al. Targeting HER2 in colorectal cancer: the landscape of amplification and short variant mutations in ERBB2 and ERBB3: ERBB2 and ERBB3 in CRC. *Cancer* 2018; 124: 1358–1373.
51. Qadir XV, Han C, Lu D, et al. miR-185 inhibits hepatocellular carcinoma growth by targeting the DNMT1/PTEN/Akt pathway. *The Am J Pathol* 2014; 184: 2355–2364.
52. Mziaut H, Henniger G, Ganss K, et al. MiR-132 controls pancreatic beta cell proliferation and survival through Pten/Akt/Foxo3 signaling. *Mol Metab* 2020; 31: 150–162.
53. Gong K, Qu B, Liao D, et al. MiR-132 regulates osteogenic differentiation via downregulating Sirtuin1 in a peroxisome proliferator-activated receptor  $\beta/\delta$ -dependent manner. *Biochem Biophys Res Commun* 2016; 478: 260–267.
54. Yao CJ, Lv Y, Zhang CJ, et al. MicroRNA-185 inhibits the growth and proliferation of osteoblasts in fracture healing by targeting PTH gene through down-regulating Wnt/ $\beta$ -catenin axis: In an animal experiment. *Biochem Biophys Res Commun* 2018; 501: 55–63.
55. Kuźbicka K, Rachoń D, Woźniowiczka A, et al. Associations of ESR1 and ESR2 gene polymorphisms with metabolic syndrome and its components in postmenopausal women. *Maturitas* 2018; 115: 97–102.
56. Wang XF, Wang YJ, Li TY, et al. Colony-stimulating factor 1 receptor inhibition prevents against lipopolysaccharide-induced osteoporosis by inhibiting osteoclast formation. *Biomed Pharmacother* 2019; 115: 108916.
57. Gao Y, Wang T, Zhang W, et al. Effect of acupotomy on chondrocyte proliferation and expression of CyclinD1, CDK4 and CDK6 in rabbits with knee osteoarthritis. *Journal of Traditional Chinese Medical Sciences* 2019; 6: 277–291.
58. Irelli A, Sirufo MM, Scipioni T, et al. mTOR links tumor immunity and bone metabolism: what are the clinical implications? *Int J Mol Sci* 2019; 20: 5841. doi: 10.3390/ijms20235841.
59. Gazitt Y, Kolaparthi V, Moncada K, et al. Targeted therapy of human osteosarcoma with 17AAG or rapamycin: characterization of induced apoptosis and inhibition of mTOR and Akt/MAPK/Wnt pathways. *Int J Oncol* 2009; 34: 551–561.
60. Chen H, Xing J, Hu X, et al. Inhibition of heat shock protein 90 rescues glucocorticoid-induced bone loss through enhancing bone formation. *J Steroid Biochem Mol Biol* 2017; 171: 236–246.
61. Massimini M, Palmieri C, De Maria R, et al. 17-AAG and apoptosis, autophagy, and mitophagy in canine osteosarcoma cell lines. *Vet Pathol* 2017; 54: 405–412.
62. Doble BW and Woodgett JR. GSK-3: tricks of the trade for a multi-tasking kinase. *J Cell Sci* 2003; 116: 1175–1186.